minerals

MDPI

Article

Remote Sensing and Mycorrhizal-Assisted Phytoremediation for the Management of Mining Waste: Opportunities and Challenges to Raw Materials Supply

Ana Rosa Castaño [1], Adalgisa Scotti [2], Vanesa Analia Silvani [3], Stefano Ubaldini [4], Francesca Trapasso [4], Emanuela Tempesta [4], Rita Rosa Plá [5], Margherita Giuffré [4], Natalia Andrea Juarez [2] and Daniela Guglietta [4,*]

[1] International Center for Earth Sciences, National Atomic Energy Commission, Malargüe 5613, Mendoza, Argentina; anaro95@gmail.com
[2] Bio Environmental Laboratory, International Center for Earth Sciences, National Atomic Energy Commission, San Rafael 5600, Mendoza, Argentina; adalgisascotti@gmail.com (A.S.); andreaj1606@gmail.com (N.A.J.)
[3] Institute of Biodiversity and Applied and Experimental Biology, Faculty of Exact and Natural Science, National Scientific and Technical Research Council—University of Buenos Aires, Buenos Aires 1428, Argentina; vanesasilvani@gmail.com
[4] Institute of Environmental Geology and Geoengineering, National Research Council of Italy (CNR IGAG), Research Area of Rome 1, 00010 Rome, Italy; stefano.ubaldini@cnr.it (S.U.); francesca.trapasso@cnr.it (F.T.); emanuela.tempesta@cnr.it (E.T.); margherita.giuffre@cnr.it (M.G.)
[5] Department of Nuclear Chemistry, GAANS, National Atomic Energy Commission, Presbítero Juan González y Aragón 15, Ezeiza B1802AYA, Provincia de Buenos Aires, Argentina; ritapla2017@gmail.com
* Correspondence: daniela.guglietta@cnr.it

Abstract: In recent times, the development of innovative processes permits the application of a circular economy approach to the management and exploitation of mining waste with respect to human health and environment, such that society is changing its fundamentally negative perception of the mining sector. This study presents the opportunities and challenges of supplying raw materials from waste using a remote sensing technique, mycorrhizal-assisted phytoremediation, and hydrometallurgical techniques to transform mining waste from a problem to a resource. Soil/mine wastes from the Sierra Pintada mine (Mendoza, Argentina) were mineralogically and chemically analyzed, and then, a mapping of the mining waste was carried out by Sentinel-2A images to identify areas with similar characteristics. The bioaccumulation of HMs by autochthonous shrubs was also determined to select accumulator plant species, and to evaluate their potential for phytoremediation of mine soils at different technological scales, when they were inoculated with arbuscular mycorrhizal fungi originated from a mining-impacted area. RMs were recovered from plant biomass by scaling in bioreactors, the depuration module, and hydrometallurgical techniques. The encouraging results highlight that this multidisciplinary approach can be applied to meet the increasing demand for RMs supply and, at the same time, to protect the environment and public health.

Keywords: Sentinel-2 image; pixel-based classification; circular economy; mycorrhizal-assisted phytoremediation; scale up-hydrometallurgical processes

Citation: Castaño, A.R.; Scotti, A.; Silvani, V.A.; Ubaldini, S.; Trapasso, F.; Tempesta, E.; Plá, R.R.; Giuffré, M.; Juarez, N.A.; Guglietta, D. Remote Sensing and Mycorrhizal-Assisted Phytoremediation for the Management of Mining Waste: Opportunities and Challenges to Raw Materials Supply. *Minerals* **2023**, *13*, 765. https://doi.org/10.3390/min13060765

Academic Editor: Michael Hitch

Received: 6 April 2023
Revised: 25 May 2023
Accepted: 31 May 2023
Published: 31 May 2023

1. Introduction

Since prehistoric times, humans have exploited their territory and its resources to their own ends (progress, competition, and economic growth) with little or no attention to the environmental, health, and social consequences. The worldwide population growth, the emerging technological development, and the high demand for raw materials (RMs) have led to an ever-less-sustainable consumption of mineral resources, since they were considered as abundant and easily extractable. During industrial processes and consumption, large quantities of waste are accumulated causing notable environmental problems associated with their disposal, including ecological losses, downstream contamination, and

pronounced landscape transformation (e.g., stockpiled waste rock and tailings, subsidence basins, open pits, and removal of overburden rock and topsoil) [1]. After the Aznalcollar (Spain, 1998) and Baia Borsa/Baia Mare (Romania, 2000) accidents involving mining activities (the latest in a long list), in 2006 the European Commission (EC) adopted the Mining Waste Directive on the management of waste from extractive industries [2].

Although European countries have a long mining history, they produce only 3% of the world's ore, but consume 25%–30% of the world's metal [3]. Over the last decades, due to increasing domestic production costs, competitive land use, and resource depletion, EU countries' RMs import rate has dramatically increased, representing one of the key challenges for the EU economy. Nevertheless, to address this major challenge, in 2008, the EC adopted the European RMs Initiative [4] and, in 2011, a strategy document [5] based on three pillars to secure and improve access to RMs for the EU: (1) ensuring the fair and sustainable supply of RMs from international markets; (2) fostering sustainable supply within the EU; and (3) boosting resource efficiency and promoting recycling. In 2011, the EC started publishing the lists of Critical Raw Materials (CRMs), defined as those RMs that are economically and strategically important for the European economy [5–8]. CRMs are identified in the EU according to two main dimensions—economic importance and supply risk—that change over time and thus the list is subject to regular reviews and updates [9], the latest dating back to 2020 (https://rmis.jrc.ec.europa.eu/, accessed on 15 March 2023).

Current EU goals are to: (i) reduce import dependency by improving access to RMs within the EU and from other sources; (ii) promote resource efficiency also through recycling and substitution; and (iii) to reduce environmental and social impacts [9]. In this context, mining waste plays a major role as these huge deposits represent, at the same time, a social and environmental concern as well as potential anthropogenic resources, exploitable through appropriate management strategies and innovative processing solutions. However, to achieve that, it is necessary to know accurate information about waste because, at the time of opening mining activity, the waste chemical and mineralogical composition was ignored, or this material was considered below the cut-off grade [10]. In the present, the technological progress and development of innovative processes permit the application of a circular economy approach to the management and exploitation of mining waste with respect to human health and environment, so that society changes its fundamentally negative perception of the mining sector [10]. During the pandemic situation linked to COVID-19 and the Ukraine war, the concern has transformed into a major problem creating a status of dependence on extra-EU supply for Europe and risks of market distortions. To overcome this problem, multidisciplinary approaches are being developed that consider the common interest towards the raw materials needed, acting sustainably and responsibly for the green recovery and for building a fair and climate-neutral economy.

To this end, in the last few decades, a remote sensing approach has been increasingly used in geological applications (such as mineral exploration) by exploiting the specific interactions of geological materials with electromagnetic spectrum in three wavelength regions: visible to near infrared (VNIR-from 400 nm to 1000 nm), shortwave infrared (SWIR-from 1000 nm to 2500), and thermal infrared (TIR- from 7600 nm to 14,000 nm) [11,12]. Thanks to the diagnostic spectral absorptions, unique for each material, the remote sensing represents a key tool to individuate and map the mining waste in a valuable, fast, low-cost, and sustainable way, and, at the same time, to manage wastes rich in RMs as resources for the future [11–13]. In particular, Sentinel-2, the European optical imaging satellite launched in 2015 as part of the European Space Agency's Copernicus Program, is used in studies to optimize the management of mining waste [14], to improve mineral estimation by band ratio [15], to map mining residues rich in RMs [16], exploiting the spatial resolution of 10–20 m, and to revisit the frequencies of 10 days and spectral resolution ranging from 490 nm to 2190 nm.

The use of biological methods to improve the quality of the environment, degraded because of anthropo-pressure, is a priority at this time [17,18]. Many studies tackle the challenge to recover RMs from mining waste by using mycorrhizal-assisted phytoremediation

(MAP) [19]. The MAP is composed of a hyperaccumulating plant species associated to an Arbuscular Mycorrhizal (AM) fungus in its roots, and the addition of an enzymatic cofactor, placed in an environment constituted by volcanic ashes and soil (methodology according to the granted patent) [20]. There are many hyperaccumulating species of heavy metal(loids) (HMs) described in the literature within the families *Asteraceae*, *Poaceae*, and *Brassicaceae*, and most of them establish mutualistic symbiosis with AM fungi (*Glomeromycota* Phylum). AM fungi are capable of uptaking nutrients and HMs from soil and translocating them to the host plant. They also accumulate these elements in the intraradical structures or immobilize them in external mycelium and spores in soil [21]. Some mycorrhized plant species show high bioaccumulation of HM in their roots, and others display high translocation and bioaccumulation in the aerial parts, with exclusion of HM from the reproductive and fruiting parts [19]. These behaviors highly depend on the plant species, the nature and concentration of the HM, the environmental and physical-chemical variables, such as the presence of other metals, and pH and Eh values in soil/substrate. The substances involved in the processes, some of them being described as the results of mycorrhizal symbiosis, are fundamentally phytochelatins (involved in HM chelation and making them more bioavailable for entry into cells), metallothioneins (that favor the entry of certain HM into cells), and glomalin (glycoproteins secreted by AM fungi that sequester HM in soils). Other transporting substances are still being studied [19,22,23].

The MAP system to be applied to the territory must go through different technology maturation stages called Technology Readiness Levels (TRLs). The TRL for pilot tests or prototypes that involve environmental engineering has nine levels, from the verification of conceptual hypotheses to the replication in territory [22,24,25]. Scotti et al. [24] proposed a Vegetable Depuration Module (VDM) for scaling up the MAP at TRL 6. The VDM falls under the definition of artificial subsurface wetland, but with the difference that it is modified in its solid matrix and in its slope with an outlet to a collecting chamber. These modifications allow us to know the partition of HMs and the possibility of recycling the filtered solution by setting other modules in series or parallel order with a change in calibration parameters [22,25].

In this work, we acquired a Sentinel-2A image to analyze a simultaneous image with the same time campaigns and we built a bioreactor (BR) that simulates the VDM at a smaller scale (TRL 4). The BR is ten times smaller than the VDM longitudinally but with the same characteristics of height, slope, and fill contents. The calibration of physical-chemical-biological variables in BR permits us to extrapolate and to verify results to the VDM (TRL 6). Additionally, any variable can be adjusted for the change in scale, and a protocol emerges to be applied in territory to the extent required by the project engineering [19,24,25]. The extraction potential of the system is related to the physical-chemical-biological variables. The hydraulic variables are related to irrigation, inflow, outflow, slope, type of vertical or horizontal flow, hydraulic retention time, and hydraulic constant. Any variation of those conditions can promote the element exclusion or bioaccumulation in plant biomass [26]. The amount of biomass obtained and the high bioextraction potential with the MAP system are essential for the recovery of secondary raw materials (SRMs) and CRMs, this is why the scaling in VDM to TRL6 is proposed.

The aims of this study were to determine the potential of Sentinel-2 for the classification and mapping of mining waste, identifying the areas in the mine with the same mineralogical, chemical, and spectral characteristics, and then to apply the MAP system followed by the hydrometallurgy technique to extract HMs of importance, in order to transform mining waste from a problem to a resource, together with the possible opportunities and challenges of exploiting wastes.

2. Materials and Methods

2.1. Study Area and Sampling Sites

The Sierra Pintada Uranium mine, with an area of 2007 Ha, is located approximately 12 km to the Southwest of Villa 25 de Mayo in Mendoza province (Figure 1). It was dis-

covered in 1968 through aerial radiometric prospecting, identifying a series of anomalies with subsequent corroboration of Uranium presence within the area. The area belongs to the so-called San Rafael Block, for the Sierra Pintada area. It is constituted by the basement of ancient lands (Devonian and Carboniferous), affected by intense tectonism and a profuse volcanic activity developed in the Lower Permian that led to the accumulation of an important sequence of volcanic clastic rocks [27]. The large volumes of intermediate and acid ignimbrites, as consequences of permo-triassic volcanism, generated favorable conditions for the concentration of Uranium deposits [28]. From 1975, the Sierra Pintada Manufacturing Mining Complex (SPMMC) was put into operation for obtaining Ammonium Diuranate as a final product, thus converting it as the largest Argentine uranium deposit to date. However, in 1997, the mining complex was forced to stop its activities due to the drop in the international price of commodities.

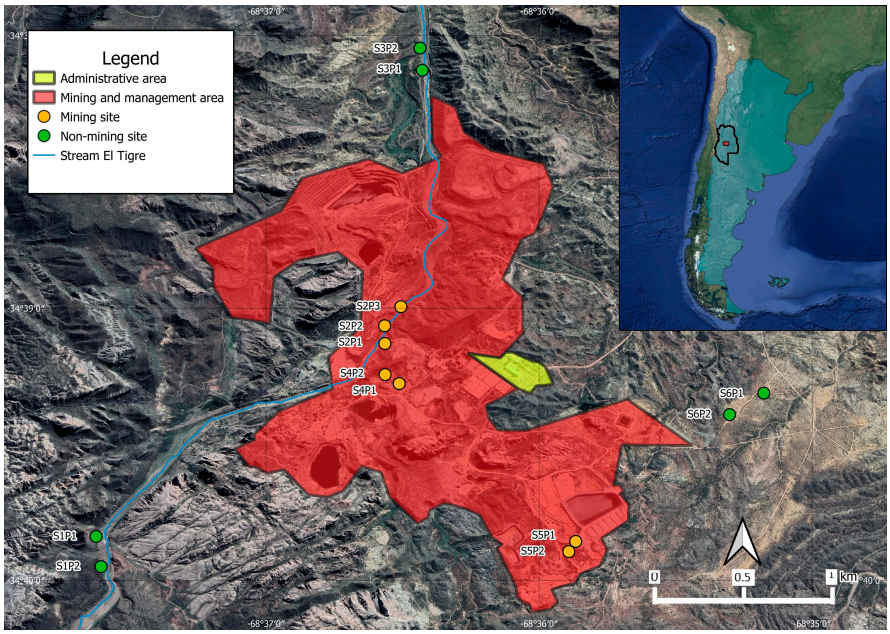

Figure 1. Study area and sampling sites in Sierra Pintada Uranium mine (Mendoza, Argentina).

In situ sampling campaigns have been carried out in December 2018 to collect samples of soil and plants of *Senecio subulatus*, (D.Don ex Hook. & Arn.), *Baccharis salicifolia* (Ruiz & Pav. Pers.), and *Senna aphylla* ((Cav.) H.S. Irwin & Barneby) (*Asteraceae* family) from 13 different sites within the mine area (Figure 1). About 1 Kg of soil sample was collected for further mineralogical and chemical characterization. Plant material was chemically determined to determine potential hyperaccumulating plant species. The geographical coordinates, pictures, and a brief description of each sampling site were registered.

2.2. Chemical and Mineralogical Analysis of Mining Waste

In the Soil Laboratory of the Uranium Mining Environmental Remediation Program (PRAMU) of the Nuclear Chemistry Department (CNEA), soil subsamples (about 50 g) were used for the determination of pH (1:3) with a Pocket Hanna Combo digital pHmeter, and the heavy metal(loids) (HMs) concentration by Neutron Activation Analysis (NAA). Previously, the samples were dried in an oven for 24 h and packed in quartz ampoules for irradiation together with the certified reference materials (NIST SRM 1633b Coal Fly Ash and Chinese Soil GBW 07405). Subsequently, the samples and the reference materials were irradiated for 4.5 h in the RA-3 reactor. Two measurements were carried out with decay times of approximately 7 and 30 days, and the following HMs were determined: As, Ce, Co, Cr, Cs, Eu, Fe, Hf, La, Nd, Rb, Sb, Sc, Sm, Sr, Th, and U. The Ortec GeHP detectors (30% efficiency, 1.9 keV resolution for the 60Co 1332.5 keV peak), the Ortec 919E multichannel buffer module and Gamma Vision data acquisition software was used. The

values of concentrations were estimated through programs developed in the laboratory. Determinations were performed using neutron activation analysis (NAA) by the Nuclear Analytical Techniques Laboratory (TAN, CNEA).

The mineralogy determination was carried out by the Institute of Environmental Geology and Geoengineering (National Research Council, Montelibretti, Italy). For that, pulverized mining wastes were analyzed with the X-Ray Powder Diffraction technique (XRPD) by using a Bruker D2 Phaser XRD, equipped with Lynxeye detector, Cu-Ka radiation and working at 30 kV and 10 mA, a fast instrument for determining the phase content of polycrystalline material. Each sample exhibited a distinctive XRPD pattern and semi-quantitative phase composition was obtained by using Crystallography Open Database of the DIFFRAC.EVA software.

2.3. Chemical Analysis of Plant Samples

Root samples and aerial parts of individual plants of *Senecio subulatus*, *Bacharis salicifolia*, and *Sena aphylla* were collected in each sampling site and the content of HMs was determined through NAA as previously described. Firstly, plant samples were ground using a cryogenic mill and lyophilized for 24 h, then, they were pelletized and packaged for irradiation, and subsequently measured. Two measurements were made with decay times of approximately 7 and 30 days for the determination of: As, Ce, Co, Cr, Cs, Eu, Fe, Hf, La, Rb, Sc, Sm, Sr, Th, U, and Zn.

2.4. Analysis of Sentinel-2A Image in the Sierra Pintada Mine Area

The spatial, spectral, and temporal resolution of satellite data together with data availability, data storage, and data handling limitations, have prevented the use of remote sensing in many potential applications. To try and overcome these limitations, the European Space Agency (ESA, Paris, France) and European Commission have developed a series of next-generation Earth Observation missions, called Sentinels, for land, ocean, and atmospheric monitoring, and each Sentinel mission is based on a constellation of satellites to provide accurate, timely, and free datasets. In this study, the multispectral Sentinel-2A image was downloaded from the ESA Copernicus Open Access hub and acquired in the Sierra Pintada mine area on 12 December 2018. The spatial resolution of the Sentinel-2A image is of 10 m in the visible and near- infrared range and 20 m in the short-wave infrared range, with spectral resolution ranging from 490 nm to 2190 nm. The 13 georeferenced samples, collected during the in situ sampling campaign, were overlaid on the satellite image and, for each sample, the spectral signature was acquired. Then, all the spectral signatures and mineralogical data were used as input for cluster analysis to obtain groups of spectrally and mineralogically similar samples. In particular, the average linkage between groups criterion (UPGMA algorithm) and Euclidean similarity index have been used. Afterwards, the supervised pixel-based classification was applied using the Spectral Angle Mapper (SAM) algorithm (see Guglietta et al. (2020) [14]).

2.5. Potential Phytoremediation of Autochthonous Plants

Plants of *Senecio subulatus*, *Bacharis salicifolia*, and *Sena aphylla* species were found in all sampling sites. These plant species are autochthonous from the study area, and they are characterized by their rapid growth and their great capacity to colonize disturbed areas by mining activity. Furthermore, considering the impact level and the possibility of quantifying the concentration of some HMs in plant biomass of these species, it was decided to use them as the MAP system.

The bioconcentration factor (BCF) and translocation factor (TF) were used to evaluate the potential phytoremediation of plants. The BCF is the concentration of HMs in total biomass (ppm)/concentration HMs in soil (ppm); TF is the concentration HMs in aerial part (ppm)/concentration HMs in roots (ppm). A BCF value higher than 1 indicated that a plant was an accumulator. TF value determines plant efficiency in HMs translocation from the root to the shoot. A plant was considered efficient in metal translocation from root to

shoot when TF was higher than 1 due to an efficient metal transport system. TF values less than 1 indicated ineffective metal transfer and suggested that these plants accumulate metals in the roots and rhizomes more than in shoots or leaves. The BCF and TF were determined for the vegetation that naturally grew in the SPMMC and the BCF of plant biomass in the BRs assay was also determined.

2.6. Mycorrhizal-Assisted Phytoremediation (MAP) in Bioreactors (BR) and Vegetable Depuration Module (VDM)

For the MAP system, the following plant species were considered: *Senecio subulatus* and *Bacharis salicifolia* plant species. They were inoculated with a mixed inoculum of mycelium, spores, and colonized root fragments composed by several AM fungi, previously isolated from Paramillos de Uspallata mine (Mendoza, Argentina). The AM fungal inoculum was obtained from a trap culture using *Medicago sativa* (L.) as host plant, isolated and propagated by Banco de *Glomeromycota* in vitro (FCEN UBA, https://bgiv.com.ar/, accessed on 12 May 2010) as described in [29].

Four BRs, placed in the Bioenvironmental Laboratory (CNEA-FRSR, Mendoza), were made with polycarbonate containers (30 cm × 60 cm and 80 cm in height and with 10 cm for the collector chamber to measure the volume/flow of the leachate generated by the substrate irrigation (Figure 2a)). Each BR was filled with three layers of stones of different granulometry. The first deeper layer (thickness of 10 cm) is represented by coarse gravel (average diameter = 10 cm); the second one (thickness of 15 cm) by medium gravel (average diameter = 5 cm); the third layer (thickness of 20 cm) by fine gravel (average diameter = 1 cm); and the upper layer (thickness of 15 cm) by mine soil samples, volcanic ashes (1:1, *v*/*v*), and 350 ppm $ZnSO_4$ (contaminated soil, CS) (Figure 2a). The control treatment was performed with commercial soil (BS). The BR and test chamber were connected to a collection chamber (10 cm × 30 cm and 80 cm deep) to collect percolated water. These BR had a relation of 1:10 with the vegetable depuration module (VDM, TRL 6), and conserved the dimensions, slope, filter layers, physicochemical (pH, Eh), and hydraulic parameters (hydraulic constant, hydraulic retention time, and vertical income flow) [19]. The depth and slope of the VDM and the BR are 80 cm and 6%, respectively. The VDM is located at the Bioenvironmental Laboratory (CNEA-FRSR, Mendoza) and a description of its performance is detailed in Scotti et al. [19] (Figure 2c). The size of VDM is 3 m in width and 5 m in length with a collection chamber of 3 m in width and 1 m in length (Figure 2b). According to Scotti et al. [25], the fill is made up of layers of coarse gravel, fine gravel, pellets, and the substrate to be bioremediated.

Figure 2. Overview of Bioreactors placed in Bioenvironmental Laboratory (**a**), VDM with vertical flow (**b**), and overview of VDM (**c**).

2.6.1. Hydraulic Parameters in BR and VDM

To model the hydraulic flow in the BR and the VDM, Darcy's law was used. This law considers the inlet and outlet flow when field capacity is reached by this Equation (1):

$$Ks = \frac{Q}{(Ac * s)}, \quad (1)$$

where

Ks: hydraulic constant (m/days);

Q: average flow rate at which it enters and which it exits (m^3/days);

Ac: perpendicular area to the flow (m^2) = 0.3 m × 0.5 m;

s: slope (m/m) = 0.03 m/0.5 m.

Furthermore, the hydraulic retention time (th) was measured by registering the time it took the flow to cross down the different layers and to exit towards the collecting chamber.

Additionally, the water-holding capacity (WHC) of the BR was determined by Equation (2):

$$\text{MWHC} = \text{Mt} - \text{Ms} \quad (2)$$

where

MWHC: mass of the water in grams;

Mt: total mass of the container and wet soil in grams;

Ms: total mass of the container and dry soil in grams.

2.6.2. Experimental Design and Measurement of Parameters

Four BR were performed, as described above, under two treatments: control soil (BS) and contaminated mine soil substrate (CS), each one inoculated by AM fungi and uninoculated. In each BR, five plants of *Senecio subulatus* and eight plants of *Bacharis salicifolia* were grown. One of the BR was inoculated with the AM fungal inocula and the other one was not inoculated. After 4 months, plants were harvested from each BR. The shoots were separated into leaves and flowers, and the roots were carefully rinsed with distilled water to eliminate substrate particles. Fresh weights of leaves, flowers, and roots were registered, then dried in an oven at 80 °C for 72 h to obtain dry biomass.

The BCF and TF were determined as previously described for the following heavy metal(loids): Cr, Zn, P, Ni, Rb, Sr, Cu, and Mn [17]. Furthermore, the BioPotential Extraction (BPBR/VDM (g)) of the system, defined as the HMs concentration in total biomass (ppm) * density of biomass plants in Br and VDM (g), was calculated.

3. Results and Discussions

3.1. Map of Characterized Mining Waste

The dendrogram of cluster analysis has identified three main groups (Cluster 1, Cluster 2, and Cluster 3) of mining waste and three samples (S3P2, S5P1, and S5P2) that do not belong to any cluster with different spectral characteristics and mineralogical phases (Figures 3 and 4). Each cluster represents a distinct class with the samples used, respectively, as training set to classify the Sentinel-2A image and as ground control point to validate the results of SAM (Figure 5). In particular, the results of accuracy include the user's accuracy (84.13%), producer's accuracy (89.6%), overall accuracy (90.73%), and kappa coefficient (0.74).

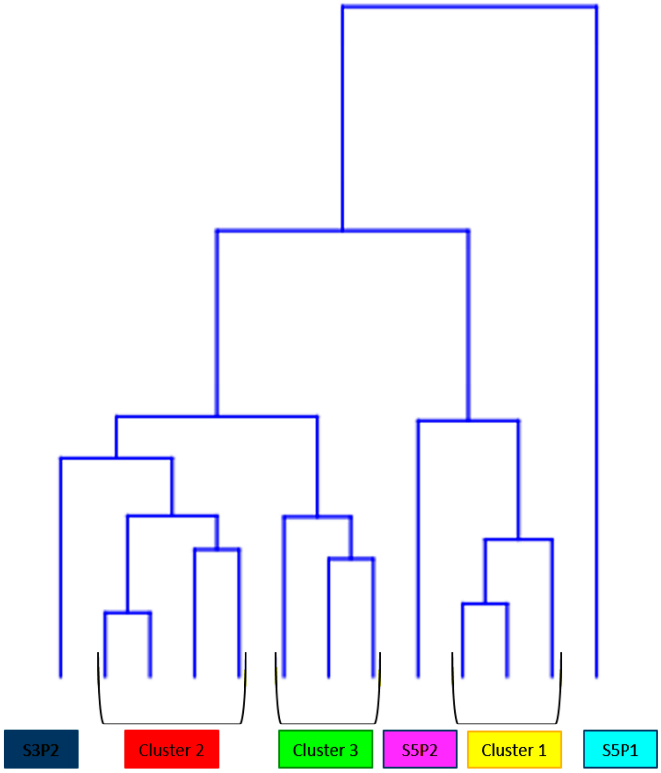

Figure 3. Cluster analysis results obtained using spectral signatures by Sentinel-2A and main mineralogical phases by Bruker D2 Phaser XRD.

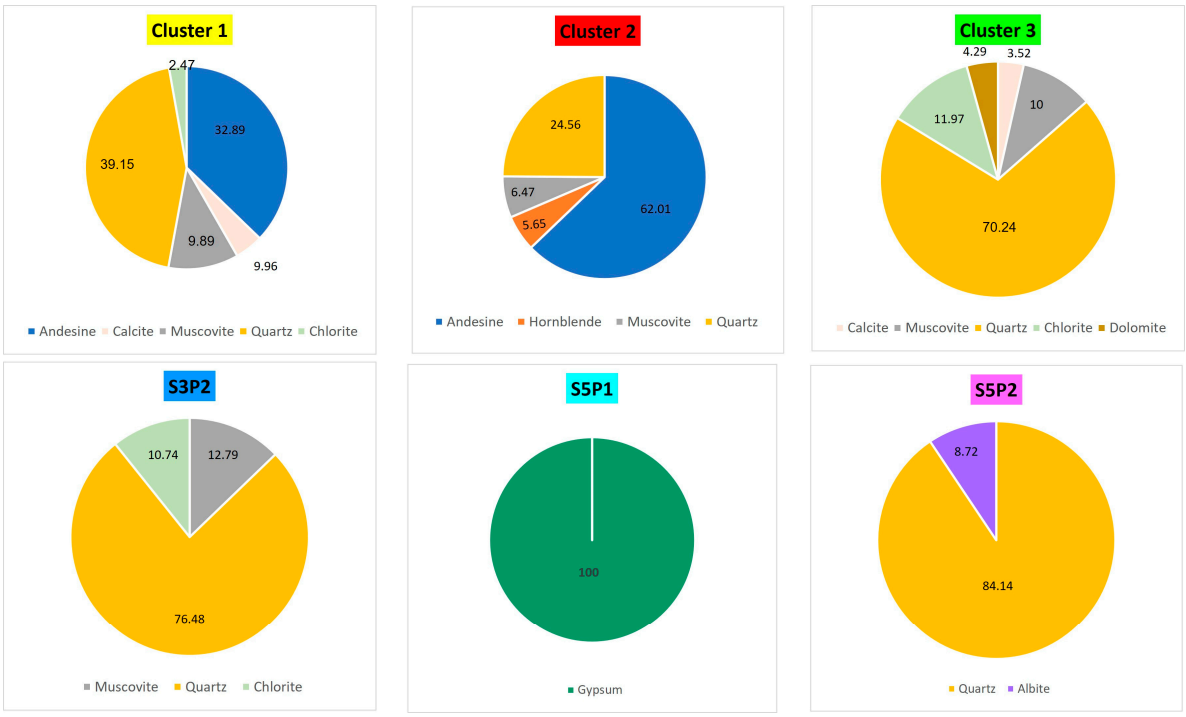

Figure 4. Concentrations of the main minerals (in percentage) in each cluster.

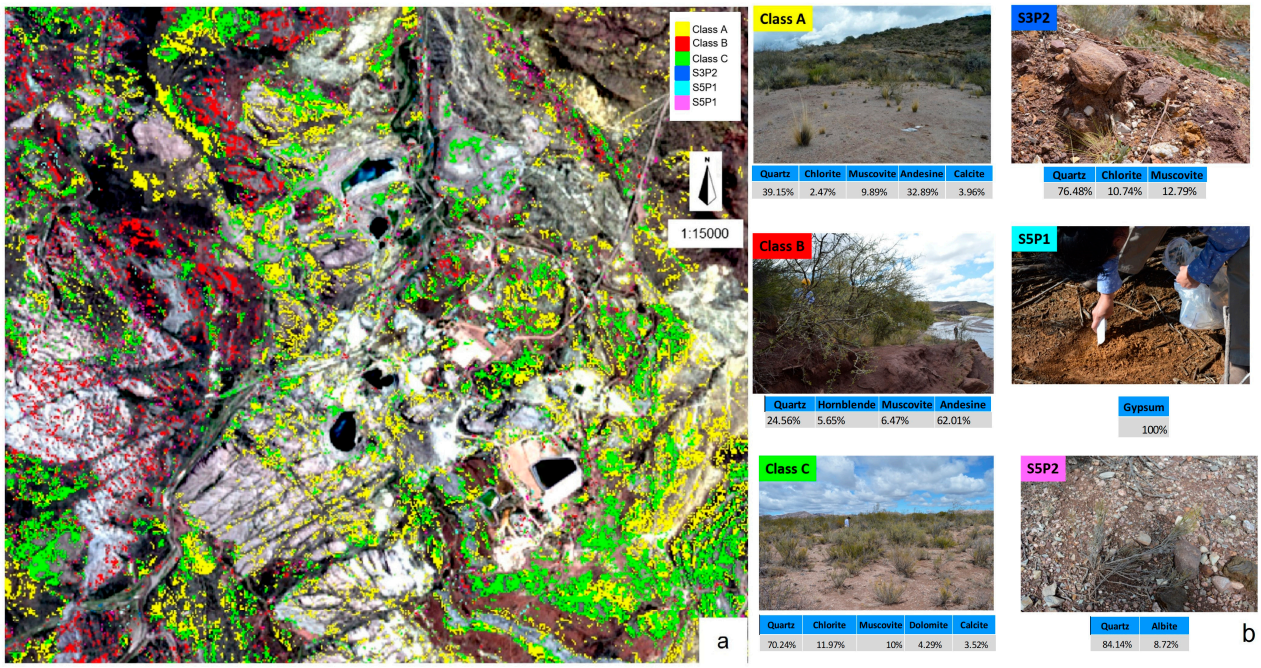

Figure 5. Map of mining waste of Sierra Pintada mine (**a**) with the description of classes and for each class the main minerals (**b**): Class A—mining waste from processing activities; Class B—samples collected in the natural area; Class C—processing waste recolonized by native vegetation; S3P2—waste from extraction process; S5P1 and S5P2—waste from processing activity accumulated over time.

The results of SAM classification have been used to create a map of mining waste that highlights the location of the classes in the Sierra Pintada mine with the major mineralogical phases (Figure 5). Class A is represented by samples from Cluster 1 (S4P1, S4P2, and S6P2) with 32.89% of andesine, 39.15% of quartz, 9.89% of muscovite, 3.96 % calcite, and 2.47% chlorite. In particular, the sample S4P1 belonging to this class derives from the processing activities of the mine, a stand with more than 20 years, with the natural native vegetation that is growing all around and the wind and water erosion processes that are accumulating material above the processing mine waste. Class B is characterized by samples from Cluster 2 (S2P3, S2P2, and S1P2) with 62% of andesine, 24.56% of quartz, 6.47% of muscovite, and 5.65% of hornblende, and this class includes the samples collected in the natural area along the Tigre River. The class C is characterized by samples from Cluster 3 (S3P1, S6P1, S2P1, and S1P1) with natural recolonization of the area by native vegetation. The main minerals are represented by quartz (70.24%), chlorite (11.97%), muscovite (10%), dolomite (4.29%), and calcite (3.52%). Furthermore, S3P2, S5P1, and S5P2, not belonging to the other three clusters, are thus different classes characterized by different mineralogical composition. S3P2 contains waste from the extraction process with 77.48% of quartz, 10.74% of chlorite, and 12.79% of muscovite. S5P1 and S5P2 have been collected in the mine area with waste from the processing mine activity accumulated over the time and with different main mineralogical phases: S5P1 with exclusively of 100% gypsum and S5P2 with quartz (84.14%) and albite (8.72%).

The map has been used to identify the different kinds of waste that are selected for further phytoremediation analysis: S4P1 from Class A (in yellow), S1P2 from Class B (in red), S2P1, S3P1, and S6P1 from Class C (in green), S5P1 (in cyan), and S5P2 (in magenta).

3.2. Potential Natural Phytoremediation

The results in Tables 1 and 2 represent the BCF and TF values for sampled vegetation grown under natural conditions at each site from the SPMMC. A value of BCF higher than 1 or close to 1 (in bold) indicates that the plant accumulated HMs in their biomass. These results support previous reports about members of the *Asteraceae* family being capable of

tolerating and accumulating large amounts of HMs and radionuclides in their tissues, and usually establishing the AM symbiosis in their roots [30].

Table 1. Total Bioconcetration Factor (BCF) of different plant species (*Senecio subulatus* (Ssub), *Bacharis salicifolia* (Ssal), and *Senna aphylla* (Saph)) sampled from the mining sites. BCF > 1 ug/g are in bold; na: not available values.

	Bioconcentration Factor in Plant Biomass															
Plant Species and Site	**As**	**Ce**	**Co**	**Cr**	**Cs**	**Eu**	**Fe**	**Hf**	**La**	**Rb**	**Sc**	**Sm**	**Sr**	**Th**	**U**	**Zn**
SsubS1P2	0.035	0.008	0.016	0.099	0.014	0.007	0.006	0.008	0.007	0.054	0.005	0.009	0.219	0.005	0.017	na
SaphS1P2	na	na	0.003	0.069	na	0.010	0.002	na	0.002	0.031	0.001	0.002	0.396	na	na	na
BsalS1P2	0.015	0.006	0.007	0.071	0.022	na	0.003	na	0.002	0.105	0.003	0.004	0.223	0.003	na	na
SaphS2P1	0.004	0.005	0.002	0.027	0.013	0.010	0.001	na	0.003	0.027	0.001	0.011	0.650	0.001	0.225	na
BsalS2P1	0.014	0.003	0.004	0.043	0.052	0.001	0.003	0.046	na	0.066	0.002	0.008	0.359	0.002	0.109	na
SsubS3P1	0.008	na	0.010	0.059	0.102	0.007	0.003	0.003	0.002	0.130	0.003	0.003	0.277	0.003	0.012	na
BsalS3P1	na	na	0.005	0.039	0.223	na	0.003	na	0.151	0.088	0.002	0.002	0.365	0.002	na	na
SsubS4P1	0.017	0.005	0.110	0.101	0.056	0.007	0.004	na	0.003	0.126	0.003	0.005	0.292	na	0.008	**31.315**
BsalS4P1	0.010	0.006	0.020	0.154	0.030	na	0.006	na	0.751	0.082	0.004	0.006	0.316	0.002	0.011	**47.547**
SaphS4P1	na	0.002	0.003	0.059	0.037	0.008	0.003	na	0.001	0.077	0.002	0.000	0.418	na	0.001	**34.143**
SsubS5P1	0.019	0.015	0.017	0.184	0.033	0.006	0.004	0.004	0.011	0.098	0.003	0.026	0.176	0.003	0.055	**11.366**
SaphS5P1	0.003	0.001	0.003	0.077	0.053	0.002	0.002	0.003	0.002	0.073	0.002	0.001	0.703	0.004	0.001	**11.984**
SaphS5P2	0.010	0.008	0.006	0.086	0.041	0.008	0.005	0.003	0.005	0.072	0.004	0.007	na	0.004	0.018	na
SsubS6P1	0.020	0.006	0.011	0.174	0.031	na	0.005	0.005	0.005	0.065	0.003	0.004	0.086	0.007	0.004	**34.104**
SaphS6P1	0.006	0.004	0.007	0.138	0.032	0.005	0.005	0.003	0.003	0.069	0.005	0.003	**1.351**	na	na	**140.067**

Table 2. Translocation factor of HMs in the different plant species (*Senecio subulatus* (Ssub), *Bacharis salicifolia* (Ssal), and *Senna aphylla* (Saph)) from the mining sites. TF > 1 is in bold; na: not available values.

	Translocation Factor in Plant Biomass															
Plant Species and Site	**As**	**Ce**	**Co**	**Cr**	**Cs**	**Eu**	**Fe**	**Hf**	**La**	**Rb**	**Sc**	**Sm**	**Sr**	**Th**	**U**	**Zn**
SsubS1P2	0.444	0.456	0.774	0.204	0.790	na	0.302	0.351	0.370	0.994	0.323	0.275	**1.192**	na	na	**1.161**
SaphS1P2	na	na	0.757	0.229	na	**1.367**	0.993	na	**1.996**	**1.538**	**1.873**	**2.188**	**1.118**	na	na	**1.860**
BsalS1P2	na	na	**1.259**	**1.463**	**2.468**	na	**3.788**	na	na	**1.789**	**8.277**	**4.050**	**1.491**	**3.261**	na	**1.033**
SaphS2P1	na	na	**2.133**	**3.576**	**1.283**	**1.741**	0.895	na	**12.27**	0.760	**4.027**	**47.14**	0.691	na	na	0.379
BsalS2P1	na	**1.099**	0.610	0.522	0.463	na	0.672	na	0.790	0.441	0.739	0.775	0.490	na	0.698	0.676
SsubS3P1	na	na	**1.341**	0.658	0.911	0.512	0.872	0.998	0.520	**1.132**	0.544	0.488	**1.689**	na	na	**2.067**
BsalS3P1	na	na	0.858	0.842	0.691	na	0.443	na	0.467	0.681	0.247	0.352	**1.138**	na	na	0.799
SsubS4P1	0.676	**2.201**	**14.352**	**1.868**	**2.543**	**3.785**	**3.323**	na	**1.979**	**1.080**	**5.647**	**1.758**	**4.277**	na	**1.510**	**3.574**
BsalS4P1	na	0.551	**2.067**	0.652	**2.126**	na	**3.029**	na	0.710	**1.842**	**5.409**	na	**2.848**	na	0.424	**3.008**
SaphS4P1	na	na	0.700	**2.076**	0.556	0.449	**1.258**	na	**1.463**	**1.171**	**1.731**	na	0.558	na	na	**1.076**
SsubS5P1	0.851	0.676	**3.389**	0.313	**3.058**	**1.493**	**1.254**	**2.448**	0.783	**3.300**	**2.916**	0.401	**1.861**	**2.528**	0.356	**2.093**
SaphS5P1	0.727	na	0.259	0.226	**2.286**	0.353	0.491	na	0.297	**2.887**	0.278	0.277	0.594	0.845	na	**3.015**
SaphS5P2	0.636	0.456	0.796	0.289	**2.582**	0.584	0.702	**1.438**	0.481	**3.367**	0.663	0.292	0.764	0.572	0.341	**4.000**
SsubS6P1	0.931	0.803	**1.059**	0.781	**1.023**	na	0.714	**1.194**	0.768	**1.056**	0.744	0.794	**1.126**	**1.363**	na	**1.017**
SaphS6P1	na	0.534	0.411	0.215	**2.821**	0.442	0.364	0.000	0.334	**3.153**	0.328	0.346	**1.172**	0.000	na	**3.923**

A high extraction potential and bioaccumulation of Zn in the biomass of the sampled plants of *Bacharis salicifolia* (BCF Zn = 47.547) from the S4P1 site (Class A), and of *Sena aphylla* (BCF Zn = 140.067) from the S6P1 site (Class C), were detected. The *Sena aphylla* plants from S6P1 (Class C) had the highest value of BFC of Sr (1.3).

Regarding the TF, the results in Table 2 indicate that the HMs passed from the roots to the aerial part when the value of TF is greater than 1, whilst a TF < 1 indicates low translocation to the aerial part, and possibly the stabilization of HMs in the roots or soil.

The highest value of TF for Co, Eu, and Sr were found in the biomass of *Senecio subulatus* grown at the S4P1 site (Class A) with 14.35, 3.78, and 4.28, respectively. The TF values for *Bacharis salicifolia* plants found at S1P2 site (Class B) were 3.78 for Fe and 4.05 for Sm.

With regards to the ability of *Sena aphylla* to translocate HMs from roots to aerial parts (Table 2), it was observed that the highest values of TF were obtained for La (12.27), Sm (47.14), Cr (3.5), Eu (1.74), and Sr (1.17) in plants grown at the S2P1 and S6P1 sites (Class C), Zn (4.0) from S5P2, and Fe (1.25) from the S4P1 (Class A) sites. For the rest of the elements, low values of TF were obtained.

In *Sena aphyla* plants from the S5P1 site, the TF values for As and Th were close to 1, and these elements could be considered as transferable in *Sena aphylla*. HMs with very low values of TF, such as U and Th (S5P2 site), Co (S5P1 site), and Zn (S2P1 site), could be stabilized in the root tissues or soil. Although the TF indicates translocation to the aerial part of *Sena aphylla* for some elements, the low BCF values indicated a weak translocation of these elements from the soil to roots, or probably a strong sequestration of HMs into the soil matrix. The efficiency of *Sena aphylla* to uptake the elements could depend on root exudates, soil pH, texture, and content of organic matter. Otherwise, soil microorganisms and AM fungi could greatly influence the sequestration and/or assimilation processes of *Sena aphylla* plants [17].

A positive correlation between the concentrations of HMs in soil with the concentrations in roots and aerial parts was detected in *Sena aphylla* plants grown at the S5P1, S5P2, and S1P2 sites (Cluster 2) (Figures 3 and 5). In the remaining sites, there was a positive correlation between the concentration of the elements in the root and in the aerial part.

The HMs concentrations in the roots of *Sena aphylla* were higher than the values in the aerial parts for Zn, Cs, La, Sc, Rb, Co, Cr, Eu, Fe, Sr, and Sm, which are transferred from the root to the aerial part while others (such as U, Th, and Co) did not, and this depended on the low value of TF (TF < 1). The results indicate that these elements are probably stabilized in the root system. *Senecio subulatus* and *Bacharis salicifolia* plants were able to translocate Sr from roots to the aerial part. This is of great importance given that Sr is considered as an RM.

According to the Total BCF (Table 2) of the studied vegetation developed under natural conditions in the SPMMC, *Senecio subulatus*, *Sena aphylla*, and *Bacharis salicifolia* had the capacity to accumulate great amounts of Zn and Sr. Figure 6 shows that the presence of Zn is only for the S4P1 (Class A), S5P1, S5P2, and S6P1 (Class C) sites. In particular, the BCF for Zn reached 47.5 in *Bacharis salicifolia* plants at the S4P1 site (Class A), and the lowest value in *Senecio subulatus* at the S5P1 site (BCF = 11.3), while *Sena aphylla* at S6P1 (Class C) resulted in the highest value (BCF = 140).

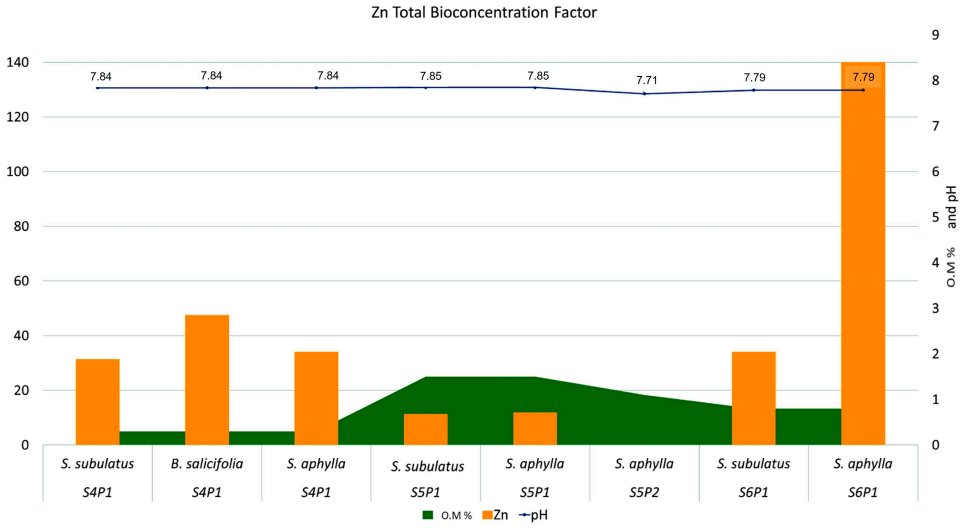

Figure 6. Total Bioconcentration factor for Zn (expressed in ug/g) in plant species found in mine sites with high Zn concentration in soil, soil pH values, and organic matter content (O.M, expressed in %).

It is noteworthy that the S4P1 (Class A) and S6P1 (Class C) sites with plants with high total BCF values of Zn (47.5 and 140, respectively), had slightly alkaline soil pH values (7.84 and 7.79) and organic matter (O.M) percentages of 0.3 and 0.8, respectively.

Figure 7 showed the total BCF for Sr in plant biomass of the three sampled plant species. It is important to note that the value of the total BCF for Sr in *Sena aphylla* biomass was higher than the other plant species. In particular, the BCF (1.35) at the S6P1 site (Class C) was higher compared to the other plant species within the same site, and the other mine sites. Furthermore, the BCF values of Sr at the S4P1 site (Class A) were equal to 0.41 *in Sena aphylla*, 0.31 in *Bacharis salicifolia*, and 0.29 in *Senecio subulatus*. At the S1P2 site (Class B), they were similar to the previous class (Class A), even if the samples were from different sites within the mining area. Class A represents mining waste from processing activities but with accumulating materials (i.e., natural rocks) on its surface by erosion processes, while Class B is characterized by samples from natural areas. The lowest values of BCF ($\leq$0.22) for Sr were highlighted in *Senecio subulatus* and *Bacharis salicifolia* plants grown at the S1P2 (Class B), S5P1, and S6P1 (Class C) mine sites.

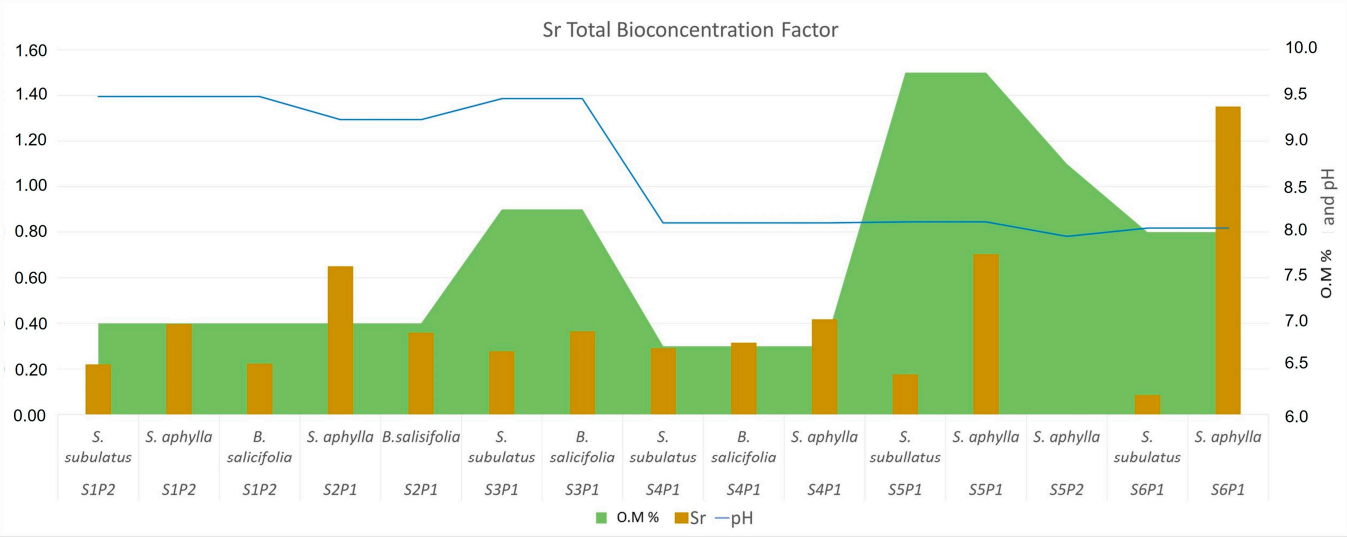

Figure 7. Total Bioconcentration Factor of Sr in biomass of plants species from different sites where it was possible to determine the value of Sr in soil with respect to pH and organic matter (O.M, expressed in %).

The O.M percentages were lower at S4P1 (Class A) site (O.M = 0.3%) and higher at the S5P1 site (O.M = 1.5%). In particular, the S4P1 (Class A) and S5P1 represent areas impacted by mining activity but with different re-vegetation processes due to site management and topographic conditions. The S4P1 site is characterized by a flat topography with a high evaporation rate, while the S5P1 is a terrain that is more uneven, with a high accumulation of soil moisture. The natural conditions of the other sites showed the typical percentages of O.M of these semi-arid zones [27].

The cluster analysis of the total BCF of HMs, the pH values, and O.M contents in soil determined clusters according to the degree of disturbance or activity related to the substrate, but also to the presence of the different plant species (Figure 8). Despite the S4P1 site being characterized by a high level of disturbance in the substrate compared to the S5P1, S5P2, and S6P1 sites, they were grouped by the HMs assimilation capacity in *Sena aphylla* and *Senecio subulatus* plants. Similar results were found with *Senecio subulatus* and *Sena aphylla* in the S5P1 site, although there was a distance between *S. aphylla* in comparison to *Senecio subulatus* in the S6P1 site (low level of disturbance). Furthermore, *B. salicifolia* in the S4P1 site was distant compared to in the S1P2, S2P1, and S3P1 sites (low level of disturbance). These results could be explained by the typical ecological behaviors

of the colonizing plant species since they usually depend on adapted mechanisms (such as competition) to establish in areas with few resources.

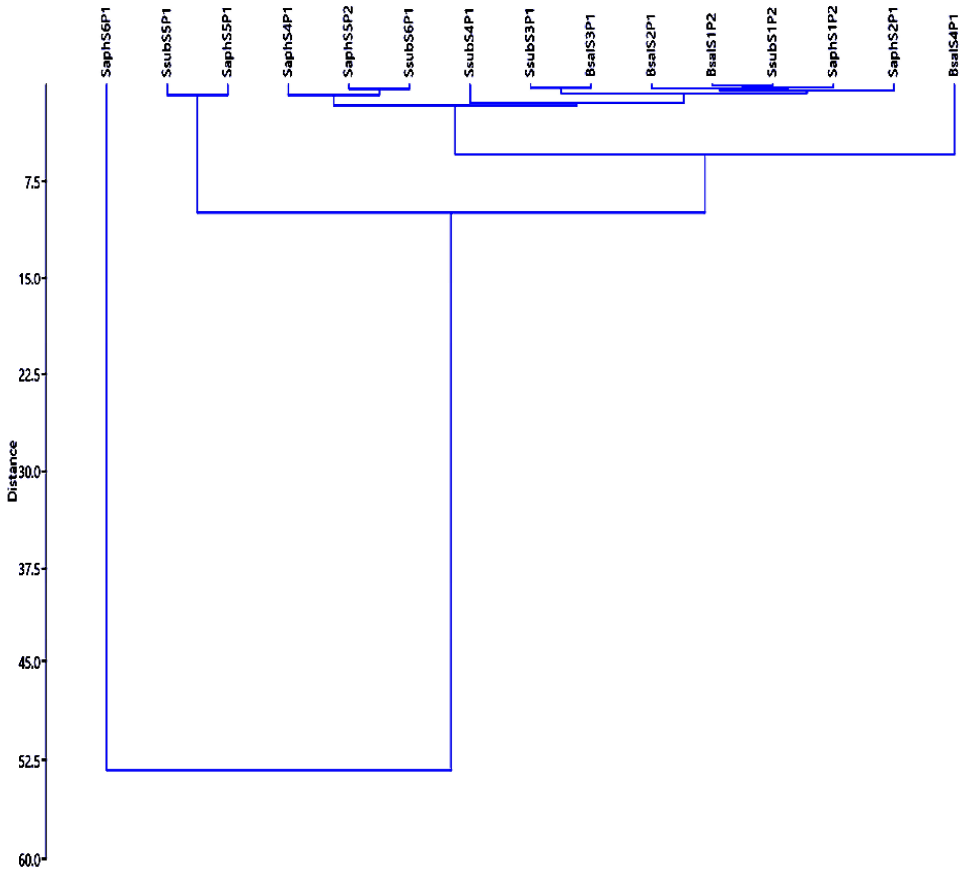

Figure 8. Cluster analysis results obtained using UPGMA algorithm and Euclidean similarity index from the total bioconcentration factor of heavy metals in the vegetation with respect to the substrate, considering the pH values and contents of organic matter (%) in each site.

3.3. Scale Up from TRL 4 to TRL 6

MAP Application in BR and Estimation of the Bioextraction Potential (BP) in VDM

Bacharis salicifolia and *Senecio subulatus* plant species were chosen for the BR experiment to recover Sr and Zn from plant biomass. Then, the results obtained in the BR were projected in the VDM. *Sena aphylla* could not be scaled in BR since it did not survive the nursery stage, even though the percentage of germinated seeds was good (300 seeds 90% germination). *Bacharis salicifolia* and *Senecio subulatus* were placed in the BR containing mining waste from the S4P1 (Class A) site (contaminated soil, CS treatment) and the other plants in BR with the control soil (blank soil, BS), under the protocol previously described. Additionally, plants were inoculated with AM fungi (M+) and other plants were not inoculated (M−). After 4 months, *Bacharis salicifolia* and *Senecio subulatus* plants developed well under BS treatment, but only *Bacharis salicifolia* grew well under CS treatment. The results of plant biomass in the BR experiment are shown in Table 3. The inoculated plants of *Bacharis salicifolia* had the highest aerial biomass.

Table 3. Biomass of *Baccharis salicifolia* and *Senecio subulatus* in aerial and roots parts, in contaminated soil (CS) and blank soil (BS) with inoculation (M+) and without inoculation (M−), of AM fungi in the BR (na: not available data; -: not survived).

Treatment	Plant Species	Aerial Tissue (Mean ± SD)	Root Tissue (Mean ± SD)
CS M+	*Bacharis salicifolia*	52.67 ± 33.53	6.75 ± 5.91
	Senecio subulatus	na	1.00 ± 0.58
CS M−	*Bacharis salicifolia*	37.67 ± 28.31	9.00 ± 7.21
	Senecio subulatus	na	na
BS M−	*Bacharis salicifolia*	30.00 ± 22.72	5.50 ± 4.20
	Senecio subulatus	48.50 ± 14.85	8.00 ± 0.00
BS M+	*Bacharis salicifolia*	35.75 ± 24.06	7.25 ± 2.87
	Senecio subulatus	82.00 ± 57.98	18.00 ± 12.73

Biological parameters such as the type of fungal inoculum MA, the plant biomass, and the physical-chemical and hydraulic parameters, such as hydraulic constant (Kh), water holding capacity (WHC), inlet flow, pH, Eh, and enzymatic cofactors, are important in carrying out scaling in the VDM and in retrieving items of interest, such as RMs. It is necessary to establish the experimental conditions of the MAP system in the BR to later scale it in VDM. In this sense, the protocol to be applied was: inflow every 2 days at field capacity, with no outlet to the collection chamber, vertical flow, mycorrhizal tension in the impacted area of the Paramillos mine, and density of 9 plants per BR. The Kh value was 165 ± 36 $m^3/d/m^2$ (mean ± SD), and the WHC resulted in 5.4 kg. These results will be considered for scaling-up in the VDM.

In previous experiments, we observed that the mentioned physical-chemical-biological variables were relevant to predict possible competitions between HMs at the membrane-cell level that could modify the patterns of entry of elements, or the presence of fungal–bacterial consortia that could exude chemical substances that alter the solubility of the different HMs present in soils [17–19]. To verify the statistical significance of the biomass obtained from the plant species in the BRs, a Tukey Test was performed (Table S1). The post hoc range test identified homogeneous subsets of means that did not differ from each other. No significant differences in the root biomass of *B. salicifolia* in the BS and inoculated (M+) and CS treatments were observed. On the contrary, the aerial parts of the plants inoculated with AM fungi (M+) of the BS and CS treatments presented more biomass than the non-inoculated one. On the other hand, the inoculated plants (M+) of *S. subulatus* had a higher biomass than the uninoculated plants of the BS treatment whilst, in contaminated soil, the plants did not survive under these conditions in the BRs. On the other hand, *S. aphylla* did not survive in the BRs.

The bioaccumulation of Sr and Zn of the studied plant species are shown in Supplemental Table S1; *Sena aphylla* was a good accumulator, followed by *Bacharis salicifolia*, and finally *Senecio subulatus* for Sr, whilst *Bacharis salicifolia* was the best bioaccumulator for Zn.

The bioextraction potential (BP) of the inoculated *Bacharis salicifolia*, previously analyzed under BR conditions, was scaled to the VDM with the following parameters: 12 plants per 0.15 m^2, 2 m^3 of substrate (soil: volcanic ash) at field capacity conditions. The projection of BP in the VDM are shown in Table 4.

Table 4. Total bioaccumulation of Zn and Sr (in ppm) in *Senecio subulatus*, *Bacharis salicifolia*, and *Senna aphylla* plant species. In parenthesis, the sampling site.

Plant Species	Bioaccumulation Sr (ppm)	Bioaccumulation Zn (ppm)
Senecio subulatus	125.5 (S4P1)	62.63 (S4P1)
Bacharis salicifolia	221 (S2P1)	95.1 (S4P1)
Sena aphylla	700.3 (S6P1)	68.26 (S4P1)

Although the three plant species resulted in a high BCF for Zn and Sr elements, only *Bacharis salicifolia* displayed adequate characteristics (resistance to manipulation, biomass)

for scaling-up in the mycorrhizal-assisted phytoremediation. Sr is considered a CRM by the fifth technical assessment in 2023 for the EU, and Zn, even if not considered critical, is important for the EU economy [3].

The MAP system was established with native plant and AM fungal species, both adapted to mine areas to efficiently extract HMs, including RMs. The results showed that the studied native species were much more efficient than non-native species associated with AM fungi from non-impacted areas. In Table 5, the BP values of Zn and Sr obtained in this experiment (678 g and 1576 g, respectively) far exceed those obtained in previous report (159 g and 30.2 g, respectively) [31]. These results may be due to the application of the AM fungal inoculum adapted to grow in metalliferous or contaminated soils that possibly show specific mechanisms for the uptake and tolerance of toxic elements [32]. Several authors have confirmed that the inoculation with AM fungi adapted to these soils increases the efficiency of bioremediation processes through greater absorption by the external mycelium and translocation to the plant, providing better protection against stress [32,33]. This result confirms the importance of AM fungal strains adapted to these conditions, for their subsequent application in degraded soils.

Table 5. Bioextraction Potential (BP) of Zn and Sr in the BR and the VDM for *Bacharis salicifolia* species.

Plant Species	Higher Total Biomass in BR	BP in BR (g)		BP in VDM (g)	
		Zn	Sr	Zn	Sr
Bacharis salicifolia	731.04	67.8	157.6	678	1576

3.4. Application of Hydrometallurgical Process

There is an increasing need to develop innovative solutions, to implement environmentally sustainable practices in the recovery of SRMs and CRMs accumulated, and to concentrate on plant biomass by application of phytoremediation techniques [19,31]. Hydrometallurgical processes have a wide range of useful applications, in the mining and environmental sector for the remediation of polluted sites, for the recovery and purification of SRMs and CRMs from wastes, and for their commercial reuse as valuable metals [19,34–39].

The results achieved in this experimental investigation encourage the subsequent recovery of SRMs and CRMs by hydrometallurgical techniques, with final purification by selective electrodeposition, as a viable environmentally friendly and cost-effective option. They allow, using specific innovative reagents and the application of electrochemical techniques, the selective recovery of precious valuable metals at high degree of purity. Therefore, following this investigation, a first phase by laboratory experiments will be carried out, assuming an integrated process circuit consisting of a leaching phase of accumulated and concentrated SRMs and CRMs, and subsequent purification by electrochemical methods. The main aim of the leaching phase will be to reach a recovery of 95% of purified metals, accumulated and concentrated on plant biomass, such as demonstrated in previous studies [19,31,37,38]. Regarding the purification phase by electrochemical methods, the scope will be to reach a purity level over 99% [37–39] that will permit an industrial reuse of SRMs and CRMs in the context of a circular economy approach. In a subsequent step, an integrated flowsheet will be drawn, with the aim of outlining a first scale-up of the process for industrial application.

4. Conclusions

Considering the actual worldwide economic and geopolitical situation, the technological advances in the field of remote sensing techniques (i.e., new sensors with high spatial and spectral resolution) and processing software, represent an opportunity to map the potential deposits of RMs, and then to supply these valuables resources from mining waste in a direct, cost-effective, and rapid way.

In this study, we have investigated the potential of Sentinel-2 to identify and classify the different types of mining waste considering similar mineralogical phases and spectral signatures, and then to create a map to recognize subjected sites for further phytoreme-

diation and extraction of RMs from mine wastes. In previous works, we applied this methodology on mining wastes of an open mine, obtaining encouraging results. In this study, we applied this methodology to the Sierra Pintada mine, a stand with more than 20 years, with different mineralogical and spectral characteristics, in comparison with mines of previous case studies.

The inoculation of plants with AM fungal species, isolated from the Paramillos de Uspallata mine, significantly improved the efficiency of the phytoextraction and bioaccumulation of autochthonous plant species. The AM fungi were found in soils with high content of Zn and Sr within the Paramillos de Uspallata mine, thus this could be related to a positive effect on these RMs by improving their bioaccumulation in the biomass of mycorrhizal autochthonous plant species. Three autochthonous plant species capable of accumulating RMs under natural conditions were chosen to optimize the bioextraction potential in the BR, through the adjustment of physical-chemical and biological parameters, prior to scaling-up to the VDM for obtaining an abundant extractive biomass of Sr and Zn. Only two plants species (*Baccharis salicifolia* and *Senecio subulatus*) were tolerant of the contamination condition of the soils and survived, but only *Bacharis salicifolia* had a good development of biomass with high extraction of RMs elements. For further studies, conditions in the BR will be optimized so that all plant species can be tested.

Finally, the remote sensing technique will be applied by multitemporal analysis from different sensors (i.e., Landsat, Sentinel-2), to highlight the process of recolonization by native vegetation in the mine and to identify the mining area for the phytoremediation process.

Supplementary Materials: The following supporting information can be downloaded at: https://www.mdpi.com/article/10.3390/min13060765/s1, Table S1. Biomass of *Baccharis salicifolia* and *Senecio subulatus* in aerial and roots parts in contaminated soil (SC) and blank soil (BS) with inoculation of AM fungi (M+) and without inoculation (M−) in the BR. Tukey HSD Test-Homogeneous group *—Ss: *Senecio subulatus*; Bs *Baccharis salicifolia*, M Mychorrized, A: aerial part, R: roots. B: blank—C: contaminated soil.

Author Contributions: Data curation, D.G., A.S., A.R.C., V.A.S., S.U., F.T., E.T., M.G., R.R.P. and N.A.J.; investigation, D.G., A.S., A.R.C. and V.A.S.; methodology, D.G., A.S., A.R.C. and V.A.S.; resources, D.G., A.S., A.R.C. and V.A.S.; writing—original draft, D.G., A.S., A.R.C., S.U. and V.A.S.; writing—review and editing, D.G., A.S., A.R.C., V.A.S. and S.U. All authors have read and agreed to the published version of the manuscript.

Funding: This research was funded by the S&T Cooperation Programme between the Italian Republic and Argentina, financially supported by the Italian Ministry of Foreign Affairs and International Cooperation (MAECI) and the Ministry of Science, Technology, and Innovation of the Argentine Republic (MINCyT), entitled: "Integrated multidisciplinary approach for the identification and recovery of raw materials from mining waste, by remote sensing". Furthermore, this work was funded by FONTAGRO ATN-RF-18951-RG 'Bioproceso reductor de la solubilidad del cadmio rizosférico'.

Data Availability Statement: Not applicable.

Acknowledgments: The authors would like to thank Veronica Iraola, Gisela Jaymes, Gabriela Coria, Vanesa Garcia, Gustavo Alvarez, and Christian Gutierrez from the National Atomic Energy Commission (CNEA, its acronym in Spanis) for their suggestion in terms of geological data and their technical support during the in situ sampling campaign.

Conflicts of Interest: The authors declare no conflict of interest.

References

1. Hudson-Edwards, K.A.; Dold, B. Mine Waste Characterization, Management and Remediation. *Minerals* **2015**, *5*, 82–85. [CrossRef]
2. European Parliament and the Council of the European Union. *Mining Waste Directive 2006/21/EC*; European Parliament and the Council of the European Union: Brussels, Belgium, 2006.
3. Bellenfant, G.; Guezennec, A.G.; Bodenan, F.; D'Hugues, P.; Cassard, D. Reprocessing of Mining Waste: Combining Environmental Management and Metal Recovery? In *Mine Closure 2013*; Tibbett, M., Fourie, A.B., Digby, C., Eds.; Australian Centre for Geomechanics: Perth, Australia, 2013.

4. European Commission. *The Raw Materials Initiative—Meeting Our Critical Needs for Growth and Jobs in Europe*; European Commission: Brussels, Belgium, 2008.
5. European Commission. *Tackling the Challenges in Commodity Markets and on the Raw Materials 2011*; European Commission: Brussels, Belgium, 2011.
6. European Commission. *On the Review of the List of Critical Raw Materials for the EU 2014*; European Commission: Brussels, Belgium, 2014.
7. European Commission. *On the 2017 List of Critical Raw Materials for the EU*; European Commission: Brussels, Belgium, 2017.
8. European Commission. *Study on the EU's List of Critical Raw Materials Final Report 2020*; European Commission: Brussels, Belgium, 2020.
9. European Commission. *Critical Raw Materials Resilience: Charting a Path Towards Greater Security and Sustainability 2020*; European Commission: Brussels, Belgium, 2020.
10. Aznar-Sánchez, J.A.; García-Gómez, J.J.; Velasco-Muñoz, J.F.; Carretero-Gómez, A. Mining Waste, and Its Sustainable Management: Advances in Worldwide Research. *Minerals* **2018**, *8*, 284. [CrossRef]
11. Van der Meer, F.D.; van der Werff, H.M.A.; van Ruitenbeek, F.-J.A.; Hecker, C.A.; Bakker, W.H.; Noomen, M.F.; van der Meijde, M.; Carranza, E.J.M.; de Smeth, J.B.; Woldai, T. Multi- and hyperspectral geologic remote sensing: A review. *Int. J. Appl. Earth Obs. Geoinf.* **2012**, *14*, 112–128. [CrossRef]
12. Buzzi, J.; Riaza, A.; García-Meléndez, E.; Weide, S.; Bachmann, M. Mapping changes in a recovering mine site with hyper spectral airborne HyMap imagery (Sotiel, SW Spain). *Minerals* **2014**, *4*, 313–329. [CrossRef]
13. Peyghambari, S.; Zhang, Y. Hyperspectral remote sensing in lithological mapping, mineral exploration, and environmental geology: An updated review. *J. Appl. Remote Sens.* **2021**, *15*, 031501. [CrossRef]
14. Guglietta, D.; Belardi, G.; Casentini, B.; Passeri, D.; Ubaldini, S.; Salvatori, R.; Trapasso, F. Optimising the management of mining waste by means Sentinel-2 imagery: A case study in Joda West Iron and Manganese Mine (India). *J. Sustain. Min.* **2020**, *19*, 4. [CrossRef]
15. Bruno, R.; Kasmaeeyazdi, S.; Tinti, F.; Mandanici, E.; Balomenos, E. Spatial component analysis to improve mineral estimation using Sentinel-2 band ratio: Application to a Greek bauxite residue. *Minerals* **2021**, *11*, 549. [CrossRef]
16. Guglietta, D.; Conte, A.M.; Paciucci, M.; Passeri, D.; Trapasso, F.; Salvatori, R. Mining residues characterization and sentinel-2a mapping for the valorization and efficient resource use by multidisciplinary strategy. *Minerals* **2022**, *12*, 617. [CrossRef]
17. Bala, S.; Garg, D.; Thirumalesh, B.V.; Sharma, M.; Sridhar, K.; Inbaraj, B.S.; Tripathi, M. Recent Strategies for Bioremediation of Emerging Pollutants: A Review for a Green and Sustainable Environment. *Toxics* **2022**, *10*, 484. [CrossRef]
18. Mocek-Płóciniak, A.; Mencel, J.; Zakrzewski, W.; Roszkowski, S. Phytoremediation as an Effective Remedy for Removing Trace Elements from Ecosystems. *Plants* **2023**, *12*, 1653. [CrossRef]
19. Scotti, A.; Milia, S.; Silvani, V.; Cappai, G.; Guglietta, D.; Trapasso, F.; Tempesta, E.; Passeri, D.; Godeas, A.; Gómez, M.; et al. Sustainable recovery of secondary and critical raw materials from classified mining residues using mycorrhizal-assisted phytoextraction. *Metals* **2021**, *11*, 1163. [CrossRef]
20. Scotti, A.; Godeas, A.; Silvani, V. Procedimiento Para Aumentar la Capacidad Biorremediadora de Plantas Hiperacumuladoras a Través de Hongos Formadores de Micorrizas Arbusculares (hma) Para Tratamiento de Suelos y/o Aguas Contaminados. Patente Argentina N° AR090183B1, 2022.
21. Colombo, R.; Benavidez, M.; Bidondo, L.; Silvani, V.; Bompadre, M.; Statello, M.; Scorza, M.; Scotti, A.; Godeas, A. Arbuscular mycorrhizal fungi in heavy metal highly polluted soil in the Riachuelo river basin. *Rev. Argent. Microbiol.* **2020**, *52*, 145–149. [CrossRef]
22. Scotti, A.; Silvani, V.; Milia, S.; Cappai, G.; Ubaldini, S.; Ortega, V.; Gómez, M. Scale-up of Mycorrhizal-Assisted Phytoremediation System from Technology Readiness Level 6 (Relevant Environment) to 7 (Operational Environment): Cost-Benefits within a Circular Economy Context. In *Book: Soil Science—Emerging Technologies, Global Perspectives and Applications*, 1st ed.; Aide, M.T., Braden, I., Eds.; Intechopen: Springfield, MO, USA, 2021. [CrossRef]
23. Ferrol, N.; Tamayo, E.; Vargas, P. The heavy metal paradox in arbuscular mycorrhizas: From mechanisms to biotechnological applications. *J. Experim. Bot.* **2016**, *22*, 6253–6265. [CrossRef] [PubMed]
24. Ibañez de Aldecoa Quintana, J.M. Niveles de madurez de la tecnología technology readiness levels: TRLS: Una introducción. *Econ. Indus.* **2014**, *393*, 165–171.
25. Scotti, A.; Cerioni, J.; Reviglio, H.; Visciglia, M.; Cerioni, S.; Biondi, R.; Saavedra, V.; Litter, M.; Silvani, V.; Godeas, A.; et al. Scaling to technological readiness levels 6 in the bio-environmental laboratory. *Robot. Autom. Eng. J.* **2019**, *4*, 555–637.
26. Mena, J.; Rodrıguez, L.; Nuñez, J.; Fernandez, F.J.; Villaseñor, J. Design of horizontal and vertical subsurface flow constructed wetlands treating industrial wastewaters. *WIT Trans. Ecol. Environ.* **2008**, *111*, 555–564.
27. Kleiman, L.E. El volcanismo permo-triásico y triásico del Bloque de San Rafael (Provincia de Mendoza): Su potencial uranífero. In Proceedings of the 12th Congreso Geológico Argentino, Mendoza, Argentina, 10–15 October 1993; Volume 5, pp. 284–293.
28. Mansilla, M.Y.; Dieguez, S.R. Modelamiento geológico mediante "software" minero del sector Tigre I. La Terraza: Distrito Uranífero Sierra Pintada, provincia de Mendoza. *Revista de la CNRA* **2013**, *51–52*, 21–31.
29. Silvani, V.A.; Fernández Bidondo, L.; Bompadre, M.J.; Pérgola, M.; Bompadre, A.; Fracchia, S.; Godeas, A.M. Growth dynamics of geographically different arbuscular mycorrhizal fungal isolates belonging to the 'Rhizophagus clade' under monoxenic conditions. *Mycologia* **2014**, *106*, 963–975. [CrossRef]
30. Ker, K.; Charest, C. Nickel remediation by AM-colonized sunflower. *Mycorrhiza* **2010**, *20*, 399–406. [CrossRef]

31. Scotti, A.; Silvani, V.A.; Juarez, N.A.; Godeas, A.M.; Ubaldini, S. The Role of Mycorrhizal-Assisted Phytomining in the Recovery of Raw Materials from Mine Wastes. *Metals* **2022**, *12*, 1828. [CrossRef]
32. Regvar, M.; Vogel-Mikus, K. Arbuscular Mycorrhiza in Metal Hyperaccumulating Plants. In *Mycorrhiza*; Varma, A., Ed.; Springer: Berlin/Heidelberg, Germany, 2008; pp. 261–280.
33. Emam, T. Local soil, but not commercial AMF inoculum, increases native and non-native grass growth at a mine restoration site. *Rest Ecol.* **2016**, *24*, 35–44. [CrossRef]
34. European Commission. *Study on the Critical Raw Materials for the EU 2023—Final Report*; European Commission: Brussels, Belgium, 2023.
35. Ubaldini, S.; Guglietta, D.; Vegliò, F.; Giuliano, V. Valorization of Mining Waste by Application of Innovative Thiosulphate Leaching for Gold Recovery. *Metals* **2019**, *9*, 274. [CrossRef]
36. Ubaldini, S.; Povar, I.; Lupascu, T.; Spinu, O.; Trapasso, F.; Passeri, D.; Carloni, S.; Guglietta, D. Application of Innovative Processes for Gold Recovery from Romanian Mining Wastes. *Chem. J. Mold.* **2020**, *15*, 29–37. [CrossRef]
37. Ubaldini, S.; Guglietta, D.; Trapasso, F.; Carloni, S.; Passeri, D.; Scotti, A. Treatment of Secondary Raw Materials by Innovative Processes. *Chem. J. Mold.* **2019**, *14*, 32–46. [CrossRef]
38. Ubaldini, S.; Massidda, R.; Veglio', F.; Beolchini, F. Gold stripping by hydro-alcoholic solutions from activated carbon: Experimental results and data analysis by a semi-empirical model. *Hydrometallurgy* **2006**, *81*, 40–44. [CrossRef]
39. Ubaldini, S.; Veglio', F.; Toro, L.; Abbruzzese, C. Combined bio-hydrometallurgical process for gold recovery from refractory stibnite. *Miner. Eng.* **2000**, *13*, 1641–1646. [CrossRef]